Vision-based approach to automated analysis of structure boundaries in scanning electron microscope images[a)]

Nak H. Kim[b)]
Department of Digital and Information Engineering, Hankuk University of Foreign Studies, Kyunggi-do, Korea

Soo-Young Lee
Department of Electrical and Computer Engineering, Auburn University, Auburn, Alabama 36849

(Received 8 July 2010; accepted 20 December 2010; published 21 January 2011)

In this article, a vision-based approach is presented for the automatic measurement of feature dimensions from cross-section scanning electron microscope images of three-dimensional structures. The cross-sections of fabricated structures are represented by a set of boundary points. The geometric distortion incurred during the imaging process is compensated for by matching the cross-section of a target structure to that of the fabricated one. Control points are defined on the boundary of the target structure, and their locations in the cross-section image are estimated using line fitting. The feature dimensions are measured based on the control points. The proposed automatic analysis method has been successfully applied to measuring dimensions of sawtooth and staircase structures transferred onto resist. *© 2011 American Vacuum Society.*
[DOI: 10.1116/1.3536505]

I. INTRODUCTION

There are numerous electronic devices that utilize three-dimensional (3-D) structures of various shapes, such as arrays of regular features, gratings, photonic band gap crystals, diffractive optical elements, magnetoresistive random access memories, and nanoelectromechanical systems.[1–3] The performance properties of these structures (devices) show high sensitivity to the dimensional measures of the fabricated structures, such as shape, size, etc. Therefore, it is often necessary to analyze the dimensional fidelity of a structure with high precision. An atomic force microscope (AFM) may be employed in measuring depth profiles from which other dimensions can be derived. However, its measurement accuracy largely depends on the sharpness of a tip and is significantly limited for structures with deep and narrow features. Another method is to use a scanning electron microscope (SEM) to obtain the image of a structure at a certain viewing angle, e.g., the cross-section of a structure viewed perpendicular to the cross-section plane.

Although a SEM is more generally applicable than an AFM, analysis of SEM images of 3-D structures has significant room for improvement. It involves tedious tasks of locating structure boundaries and measuring feature dimensions, which may lead to substantial measurement errors, especially if done manually. Certain SEMs are equipped with software that measures the size of a feature by detecting peaks (of brightness) in a SEM image. However, such measurements are mainly for two-dimensional (2-D) or binary patterns, e.g., measurement of the top-view of a pattern. Also, off-line analysis of SEM images has been studied by various researchers.[4,5] Their investigations have been centered at the conventional image processing or computer vision issues such as noise reduction, feature extraction, etc.

In a SEM image, the structure boundary appears brighter than the rest of the image. What makes edge location uncertain is the edge bloom leading to an offset in the measured edge location. There have been a number of techniques exploited for improving the localization accuracy. Recently, a model-based library approach was proposed.[6,7] The intensity profiles of various edge patterns in SEM image are stored in the library, and the measured edge profile is compared with each of the model patterns to determine the edge location. This technique has been applied successfully to determining the width of resist line, and the accuracy has been analyzed in detail. However, it needs to be pointed out that their focus was on determination of individual edge points from one-dimensional (1-D) intensity signals. Derivation of structural shapes from a set of edge points, considering the relationship among the edge points, was not addressed.

Another problem associated with using a SEM is the geometric distortion of images due to nonideal sample orientation. The nonlinearity and asymmetry often encountered in the SEM imaging process may also contribute to the geometric distortion. The issue of geometric correction was considered in an effort to facilitate accurate measurements in SEM images.[8] A piecewise affine transform was used to correct geometric distortions due to the rotation and tilt of a sample. The transform matrix is derived using a set of control points known in both the reference and distorted SEM images. Then, each pixel in the distorted image is mapped onto the corrected location through the transform. The correction method, while generally applicable, was developed for a specific type of 2-D pattern, i.e., a regular 2-D array of features

[a)]This paper was presented at the 54th International Conference on Electron, Ion, and Photon Beam Technology & Nanofabrication Conference held in Anchorage, AK, June 1–4, 2010.
[b)]Electronic mail: nhkim@hufs.ac.kr

such as circles and squares. Also, it requires that the correspondences of control points between the reference and distorted images are known.

In this study, a vision-based approach has been developed for the automatic determination of structural shapes and measurement of feature dimensions from cross-section SEM images. Certain critical points in a structure, such as peaks, troughs, and corners of features, may be utilized in this approach since it is usually difficult to localize landmark points accurately on linear or smooth sections of feature boundaries. However, during the nonideal fabrication process, such critical points are often smoothed out. Also, it is difficult to localize the critical points in images reliably.

The proposed approach first detects the boundary points of structures in the cross-section SEM image, then matches the cross-section of the target structure to the detected boundary points while compensating for any geometric distortion, and subsequently measures feature dimensions using control points set on the structure boundary. By minimizing human involvement, analysis of SEM images of 3-D structures can be made more systematic and accurate. The first implementation of the approach is tuned for sawtooth and staircase structures, although it can handle any shape.

It should be clear that our work is different from the previous research where the main emphasis is placed on the accurate localization of step edges from 1-D intensity profiles of SEM images. That is, the primary concern of our work is to derive the 2-D description of structural shape from the detected edge points and line segments and match it to the target shape by compensating for the geometric distortion due to the nonideal orientation of the sample.

This paper is organized as follows. In Sec. II, a method for detecting structure boundaries in SEM images is described. In Sec. III, a method for matching the target and fabricated structures is depicted. In Sec. IV, a procedure to measure the feature dimensions is described. In Sec. V, the results obtained for the test structures are provided with detailed discussion, followed by a summary in Sec. VI.

II. DETECTION OF STRUCTURE BOUNDARIES

A typical SEM image of a 3-D structure (sawtooth) transferred onto resist is shown in Fig. 1(a) where it can be seen that the structure boundary is blurred. The cross-section of the intended sawtooth structure is shown in Fig. 1(b); a horizontal line is added to the bottom of the structure boundary for shape matching purposes. We will refer to the intended shape of the cross-section as the *target structure* and the transferred shape of the cross-section [Fig. 1(a)] as the *fabricated structure*. Small dots in the target structure represent control points defined for enabling automatic measurement of dimensions. After the target structure is registered (matched) with the boundary points detected in the SEM image, these control points are localized in the image, and feature dimensions are computed using the measured coordinates. For instance, the depth of the structure in Fig. 1(b) can be estimated from the measured distance between points A and B.

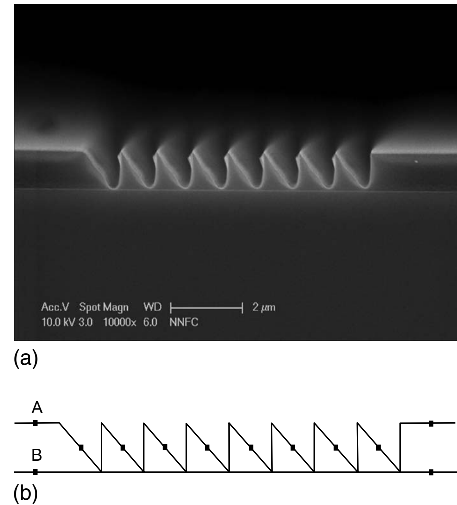

FIG. 1. (a) Cross-section SEM image of a sawtooth structure fabricated in the substrate system of 1000 nm polymethyl methacrylate (PMMA) on Si through electron-beam lithographic process (lithography). The beam energy was 50 keV and the sample was developed for 30 s in (a) the developer of MIBK:IPA=1:1 and (b) the target sawtooth structure where both the width and height of each tooth are 1000 nm.

Since the proposed approach relies on the registration of the target structure to the boundary points, the first step is boundary detection. Although edge detection techniques have been widely utilized for boundary detection, these techniques are not effective for SEM images since the image intensity variation around the structure boundary does not exhibit the step edge profile. Nevertheless, from the SEM image, it can be seen that the boundary region tends to appear brighter than other areas. When the target structure has a step edge profile, it is possible to approximate the boundary intensity pattern using some known shapes such as a sigmoid function or a set of line segments to locate the exact boundary position. However, the boundary profile in Fig. 1 is far different from such shapes.

Thus, we have utilized a peak detection technique for locating boundary points as follows. First, in order to reduce noise, we apply Gaussian smoothing to the SEM image. The spatial constant of the Gaussian filter is around one pixel. Second, the gradient is computed at each pixel to determine the local direction around it. Depending on the gradient direction, either vertical or horizontal peak detection is applied. For horizontal peak detection, a pixel is marked as a boundary point if it has a higher intensity value than both of its horizontal neighbors. Vertical peak detection is performed likewise. Finally, after detecting boundary points, a square median filter is applied to remove isolated noisy boundary points.

Depending on the orientation of the sample, in some SEM images, the cross-section area of the structure appears brighter than the dark background (see Fig. 5, for example). In this situation, a simple binary thresholding technique followed by boundary detection can locate the boundary points more accurately. For this kind of SEM image, we utilize the

binary thresholding technique. Thus, we apply the peak detection or thresholding technique, depending on the type of image.

It is known that the peak location of edge bloom is slightly different from the actual boundary, although the offset tends to be nearly constant at the boundary in the given image. Thus, when the peak detection is utilized to locate boundary points, the bias may affect the accuracy of the measured shape parameters.

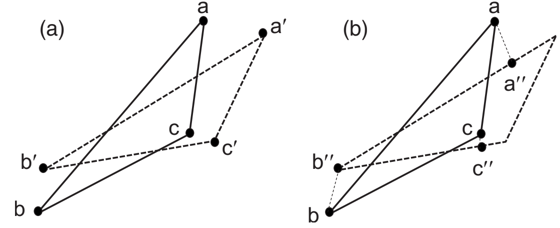

FIG. 2. (a) Exact correspondence and (b) nearest-point correspondence.

III. SHAPE MATCHING (REGISTRATION)

A. 2-D modeling of distortion

The objective of this study is to enable automatic and accurate dimensional measurement of the cross-section shape of a 3-D structure from its SEM image. An automatic measurement system usually tries to extract critical points such as peaks, troughs, and corners of shapes and to measure distances between such points, since it is usually hard to place landmark points accurately on linear or smooth sections. Our approach is to define control points on the target structure and find the locations of control points on the fabricated structure by registering the target and fabricated shapes. Under ideal conditions, the cross-section shape of the fabricated structure would match that of the target structure. However, because of various factors involved in the fabrication and imaging processes, there can be a significant difference between the two shapes, as can be seen in Fig. 1. For example, the optical axis may not be normal to the image plane, leading to foreshortening.

Thus, in this study, the shape difference between the target and fabricated structures is dealt with by deriving a relationship between them. More specifically, the image distortion is modeled using three parameters in 2-D space: two scaling factors and one rotation angle. Note that instead of modeling the tilting angles of the optical axis, the foreshortening distortion caused by the tilting angles is modeled by scaling factors in the image plane.

Let the 2-D coordinates for the target structure be given by $(u,v)^T$ and the image coordinates for the fabricated structure be given by $(u',v')^T$. It is assumed that the two coordinates are related as follows:

$$\begin{pmatrix} u' \\ v' \end{pmatrix} = \begin{pmatrix} \cos\theta & -\sin\theta \\ \sin\theta & \cos\theta \end{pmatrix} \begin{pmatrix} s_x & 0 \\ 0 & s_y \end{pmatrix} \begin{pmatrix} u \\ v \end{pmatrix} + \begin{pmatrix} t_x \\ t_y \end{pmatrix}, \tag{1}$$

where s_x and s_y are scaling factors in the horizontal and vertical dimensions, respectively; θ is the rotation angle in the image plane; and t_x and t_y denote translations in the horizontal and vertical directions, respectively.

The target and the fabricated structures are matched in the presence of distortions described by Eq. (1). In theory, if the correspondences of three noncollinear points between the two structures are established, the five unknown parameters in Eq. (1) can be found. However, since the boundary of the fabricated structure is significantly different from that of the target one as can be seen in Fig. 1, the distortion parameters are recovered by aligning the target and fabricated boundaries instead of using the point correspondences. A shape matching procedure for the alignment has been developed based on the iterative closest point (ICP) method.

B. Shape registration using ICP method

The iterative closest point method[9,10] is a registration technique, which has been used for the registration of range data. This method can find the geometric relationship between two different sets of 3-D data using an iterative procedure. Suppose that two sets of data points $\mathbf{x}$ and $\mathbf{x}'$ satisfy $\mathbf{x}'=R\mathbf{x}+\mathbf{t}$, where R is the rotation matrix and $\mathbf{t}$ is the translation vector. The registration problem is to find R and $\mathbf{t}$ from $\mathbf{x}$ and $\mathbf{x}'$.

The key idea of the ICP method lies in the way of finding corresponding points between two data sets. Instead of the exact correspondence, the nearest point is selected as the match, as illustrated in Fig. 2. The two triangles in Fig. 2(a) represent the same shape with two different orientations. The three points a, b, and c in the solid-line triangle correspond, respectively, to points a′, b′, and c′ of the dotted-line triangle. If these correspondences are established, the geometric relationship between two triangles can be computed. However, the structural deformation in fabrication, the foreshortening in SEM imaging, and the digital nature of the SEM image often make the true correspondences hard to establish.

Given a point, the nearest point in the search domain is selected as a tentative match in each iteration of the ICP algorithm. For instance, in Fig. 2(b), points a″, b″, and c″ are the nearest points of a, b, and c, respectively. These points are found by searching the neighborhood of each point. Note that the geometric distortion tends to be small in most cases since the SEM operator usually tries to make the optical axis as normal to the cross-section of structure as possible. Using these correspondences, a transformation between two data sets is computed. If one of the data sets is transformed using the computed relationship, the average distance between the corresponding points of two data sets becomes smaller. By repeating this process, the estimated transformation can be made more and more accurate. The ICP method has been applied successfully to many problems such as 3-D shape registration[11] and matching of environmental maps.[12]

ICP algorithm: Finding registration

(1) Set initial R' and $\mathbf{t}'$.
(2) Set $E \leftarrow \infty$.

(3) Repeat the following:

(a) $E_{\rm old} \leftarrow E$.
(b) For each point $\mathbf{x}_i$, compute $\mathbf{x}_i'' = R'\mathbf{x}_i + \mathbf{t}'$.
(c) Among the set $\mathbf{x}'$, find the nearest point of $\mathbf{x}_i''$ and call it $\mathbf{x}_i'$.
(d) Using the set of correspondences $\{\mathbf{x}_i, \mathbf{x}_i'\}$, compute the new transformation R' and $\mathbf{t}'$. Set E as the mean distance between corresponding points.
(e) If $|E - E_{\rm old}| < \tau$, terminate the procedure.

In step (3d), the new transformation is computed as follows. Suppose that we have n correspondences $\{\mathbf{x}_i, \mathbf{x}_i'\}$ (where $i = 1, 2, \ldots, n$) between the two data sets. The matching error can be defined by

$$E = \sum_{i=1}^{n} |\mathbf{x}_i' - R'\mathbf{x}_i - \mathbf{t}'|^2. \tag{2}$$

The translation minimizing the error should satisfy

$$\frac{\partial E}{\partial \mathbf{t}} = -2 \sum_{i=1}^{n} (\mathbf{x}_i' - R'\mathbf{x}_i - \mathbf{t}') = 0. \tag{3}$$

Let $\bar{\mathbf{x}} \equiv (1/n)\Sigma_{i=1}^{n}\mathbf{x}_i$ and $\bar{\mathbf{x}}' \equiv (1/n)\Sigma_{i=1}^{n}\mathbf{x}_i'$. Then, from Eq. (3),

$$\mathbf{t}' = \bar{\mathbf{x}}' - R'\bar{\mathbf{x}}. \tag{4}$$

Thus, once the rotation is computed, the translation can be found from Eq. (4).

Now, incorporating Eq. (4) into Eq. (2) and letting $\mathbf{y}_i = \mathbf{x}_i - \bar{\mathbf{x}}$ and $\mathbf{y}_i' = \mathbf{x}_i' - \bar{\mathbf{x}}'$, Eq. (2) becomes

$$E = \sum_{i=1}^{n} |\mathbf{y}_i' - R'\mathbf{y}_i|^2. \tag{5}$$

Let the rotation angle be θ and define

$$\tilde{R} \equiv \begin{pmatrix} \cos\frac{\theta}{2} & -\sin\frac{\theta}{2} \\ \sin\frac{\theta}{2} & \cos\frac{\theta}{2} \end{pmatrix}.$$

Then $R' = \tilde{R}\tilde{R}$, and since $\tilde{R}^T\tilde{R} = \tilde{R}\tilde{R}^T = I$, where I is the identity matrix, Eq. (5) becomes

$$E = \sum_{i=1}^{n} |\mathbf{y}_i' - R'\mathbf{y}_i|^2 = \sum_{i=1}^{n} |\tilde{R}^T\mathbf{y}_i' - \tilde{R}\mathbf{y}_i|^2. \tag{6}$$

Let $\alpha = \cos(\theta/2)$ and $\beta = \sin(\theta/2)$, and let $\mathbf{y}_i' \equiv (u_i', v_i')^T$ and $\mathbf{y}_i \equiv (u_i, v_i)^T$. Then from Eq. (6),

$$E = \sum_{i=1}^{n} |A_i\mathbf{q}|^2 = \mathbf{q}^T B \mathbf{q}, \tag{7}$$

where

$$A_i = \begin{pmatrix} u_i' - u_i & v_i' + v_i \\ v_i' - v_i & -u_i' - u_i \end{pmatrix},$$

$\mathbf{q} = (\alpha, \beta)^T$, and $B = \Sigma_{i=1}^{n} A_i$.

Thus, the problem becomes finding the vector $\mathbf{q}$ minimizing Eq. (7) subject to $|\mathbf{q}|^2 = 1$, for which the solution is the eigenvector of B associated with the least eigenvalue. Once $\mathbf{q}$ is found, the rotation matrix R' is determined, and the translation $\mathbf{t}'$ can be found from Eq. (4).

C. Scaling factors

With the ICP method, it is possible to estimate the error of the registration. This can be utilized to estimate the two scaling factors. The basic idea is to repeat the ICP registration for each possible combination of scaling factors s_x and s_y and to compute the residual error in each iteration. The factors which minimize the residual error are found through iterations. The range and the sampling interval of the scaling factors may affect the accuracy and the computation time. The choice of such parameters can be guided depending on the imaging condition and the shape of target structure. However, a few tens of trial steps for each scaling factor should suffice in most applications.

IV. MEASUREMENT OF SHAPE PARAMETERS

The target and fabricated structures can be matched to each other through coordinate transformation [Eq. (1)] using the distortion parameters. In addition to the boundary contour of the cross-section itself, quantitative dimensional measures of the fabricated structure are also needed, which are referred to as *shape parameters*. The shape parameters to be measured in this study are the various distances between certain points. For instance, in Fig. 1, one may want to measure the height of a tooth or the distances between adjacent teeth. In order to derive an automatic and reliable measurement process, a line fitting technique is employed on the predefined control points as follows.

A set of control points is defined on the structure boundary on which the desired shape parameters can be measured. Figure 1(b) shows the control points defined on the target structure of the sawtooth in Fig. 1. The height of the sawtooth structure can be determined by measuring the distance between points A and B. The distances between teeth can be measured using the control points as well. After the target structure is registered with the detected boundary points, the control points can be located in the SEM image. The detected boundary may exhibit irregularities, such as discontinuity, around a control point, which makes its location uncertain. Thus, line fitting is performed around the control point, and the point on the line closest to the control point is marked as its location.

V. EXPERIMENTAL RESULTS

Two different 3-D structures, a sawtooth and a staircase, were fabricated, and the SEM images of their cross-sections have been analyzed. Boundary points of the sawtooth structure in Fig. 1 were detected using the peak detection technique, and the detected boundary is shown in Fig. 3(a). The registration process was then applied to the detected boundary points using the ICP method, and the result is shown in

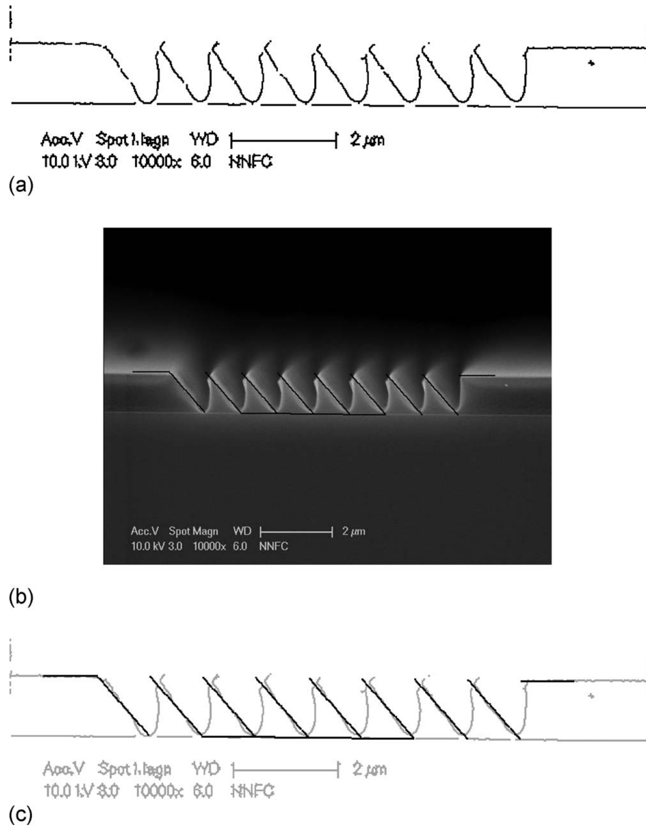

FIG. 3. (a) Detected boundary of the sawtooth structure, (b) the transformed target structure overlaid on the SEM image, and (c) the transformed target structure overlaid with the detected boundary.

Fig. 3(b) where the black lines represent the transformed target shape. Note that, besides the sawtooth structure, a part of the line (corresponding to the top surface of Si) beneath the structure is included in the target shape. The purpose of this inclusion is to avoid the ill-conditioned matching which may occur during the registration process. It can be seen that the transformed target shape has been registered well with the fabricated structure.

The distortion parameters estimated during the registration process are $s_x = 1.06$, $s_y = 1.16$, and $q = -0.70°$. In order to find the shape parameters, the locations of the control points are detected as shown in Fig. 4 where the small dots represent the detected locations of the control points.

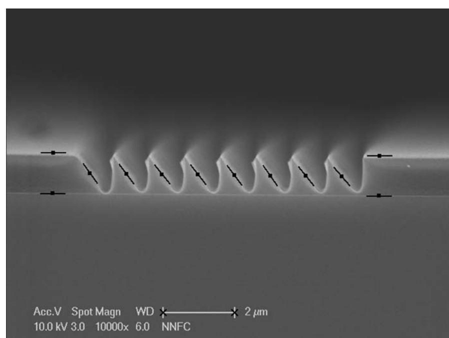

FIG. 4. Control points on the SEM image.

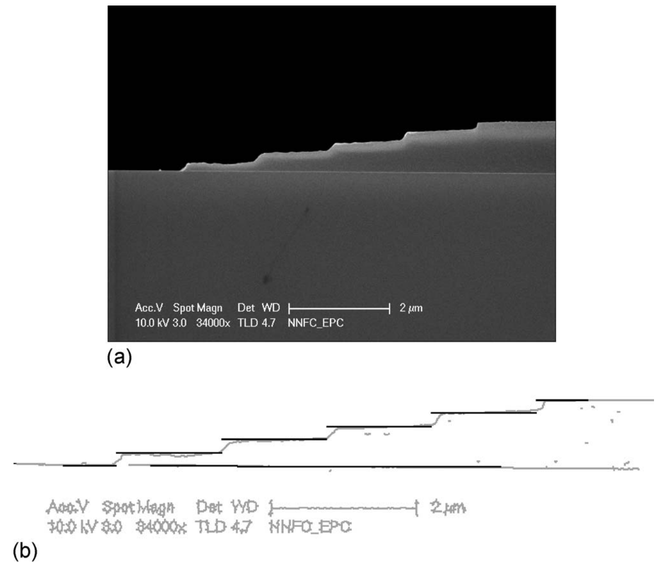

FIG. 5. (a) Cross-section SEM image of a staircase structure fabricated in the substrate system of 1000 nm PMMA on Si through electron-beam lithographic process. The beam energy was 50 keV and the sample was developed for 30 s in the developer of MIBK:IPA=1:1 and (b) the transformed target staircase structure overlaid with the fabricated structure (see Fig. 1 comments).

To enable automatic measurement, the two end-points of the scale marker are extracted as shown in Fig. 4. These points were detected automatically using a simple horizontal line search followed by a vertical bar detection process. The detected magnification factor is 57.5 pixels/μm. Under this magnification, the interpixel distance in the image is 17.4 μm. Thus, half-pixel uncertainty in the measurement amounts to 8.7 μm. Using the detected image coordinates of the control points, we measured the depth of the sawtooth structure and the distances between adjacent teeth. The measured depth was 1.03 μm, and the distances were 1.01–1.03 μm with the average width of 1.02 μm.

The SEM image of the staircase structure is shown in Fig. 5(a). Since the structure area has a distinct brightness compared with the dark background, the structure boundary was detected using a gray-level thresholding technique. However, because we also need to extract the scale marker, the peak detection was also performed. The two results were then merged. Conflicting boundary points are rejected by removing points obtained by peak detection located within the vicinity of points detected by thresholding. The detected boundary points overlaid with the transformed target structure are shown in Fig. 5(b).

The control point locations are then detected as shown in Fig. 6 where the end-points of the scale marker are shown as

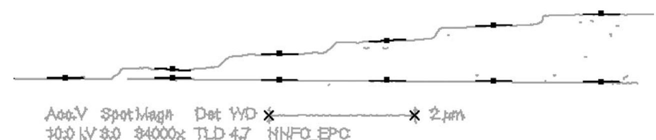

FIG. 6. Control points on the structure boundary and scale marker.

well. Using the measured coordinate information, the heights of the five steps were calculated to be 0.18, 0.2, 0.21, 0.23, and 0.12 μm from the top to the bottom layer, respectively.

It needs to be pointed out that the accuracy of the feature dimensions measured by the proposed method can be affected by any uncertainty in the boundary location, although this uncertainty is not what is to be addressed by this study. An earlier study[6] indicated that the offset of edge location, which is due to the edge blooming in SEM images, can be about 5 nm. Assuming the same offset, the worst case uncertainty in the measured feature dimensions would be about 10 nm. While this is true in general, for certain measurements such as feature interval, step height in a staircase, etc., the uncertainty would be much less or even almost zero since the offsets tend to cancel each other.

The computational requirement of the proposed method varies depending on factors such as the image size, the number of target points, and the number of repetitions with varying scaling factors as described in Sec. III C. The nonoptimized code requires about 5–6 s of computation time for the SEM images (size: 723×543 and 714×486 pixels), analyzed in this study on a PC with an Intel Core2Duo processor (2.53 GHz) in a Windows environment.

VI. SUMMARY

A vision-based method for the automatic analysis of cross-section SEM images of 3-D structures, developed to avoid manual measurement, is described in this article. The method employs a peak detection or thresholding technique for boundary detection, a registration process for extracting distortion parameters, and a set of control points for measuring the shape parameters. In the registration process, the ICP algorithm is adopted. The first implementation of the proposed method has been successfully tested for sawtooth and staircase structures. Since there is no specific assumption on the shape of a structure, it is expected that the proposed approach can be applied to other shapes as well.

[1] C.-H. Chang, R. K. Heilmann, R. C. Fleming, J. Carter, E. Murphy, M. L. Schattenburg, T. C. Bailey, J. G. Ekerdt, R. D. Frankel, and R. Voisin, J. Vac. Sci. Technol. B **21**, 2755 (2003).
[2] B. Morgan, C. Waits, J. Krizmanic, and R. Ghodssi, J. Microelectromech. Syst. **13**, 113 (2004).
[3] T. Bourouina, T. Masuzawa, and H. Fujita, J. Microelectromech. Syst. **13**, 190 (2004).
[4] S. K. Alexander, R. Azencott, B. G. Bodmann, A. Bouamrani, C. Chiappini, M. Ferrari, X. Liu, and E. Tasciotti, *Computer Analysis of Images and Patterns*, Lecture Notes in Computer Science (Springer, Berlin, 2009), Vol. 5702, pp. 590–597.
[5] Y. Midoh, K. Nakamae, and H. Fujioka, Meas. Sci. Technol. **18**, 579 (2007).
[6] J. S. Villarrubia, A. E. Vladár, B. D. Bunday, and M. Bishop, Proc. SPIE **5375**, 199 (2004).
[7] J. S. Villarrubia, A. E. Vladár, and M. T. Postek, J. Microlithogr., Microfabr., Microsyst. **4**, 033002 (2005).
[8] J. Kapur and D. Casasent, Proc. SPIE **4044**, 165 (2000).
[9] P. Besl and N. McKay, IEEE Trans. Pattern Anal. Mach. Intell. **14**, 239 (1992).
[10] D. A. Forsyth and J. Ponce, *Computer Vision: A Modern Approach* (Prentice-Hall, Englewood Cliffs, NJ, 2003).
[11] G. Turk and M. Levoy, Proc. SIGGRAPH 311 (1994).
[12] F. Lu and E. Milios, J. Intell. Robotic Syst. **18**, 249 (1997).